

Electronic Supplementary Information

Synthesis of hyperbranched polyarylethenes by consecutive C–H vinylation reactions

Anastasia Yu. Gitlina,^a Albert Ruggi,^b and Kay Severin^{*a}

^a Institut des Sciences et Ingénierie Chimiques, École Polytechnique Fédérale de Lausanne (EPFL), 1015 Lausanne, Switzerland

^b Département de Chimie, Université de Fribourg, 1700 Fribourg, Switzerland

Table of contents

| | |
|---|-----|
| Materials and methods | S2 |
| Synthesis of the polymers | S3 |
| Mass spectra | S5 |
| NMR spectra | S9 |
| Thermogravimetric analyses of the polymers | S12 |
| Photophysical properties | S13 |
| Aggregation-induced emission of the polymers | S19 |
| Sensing of the cations | S24 |
| CIE chromaticity diagrams | S28 |
| DLS measurements | S29 |
| Optimization of the reaction conditions | S30 |
| References | S33 |

Materials and methods

Unless otherwise stated, all chemical reactions were carried out in oven-dried (110 °C) glassware under an atmosphere of dry N₂ using Schlenk or Glovebox (MBraun) techniques. All reagents and solvents were purchased from chemical suppliers (Sigma Aldrich, Fluorochem, Acros Organics, TCI, Apollo, ABCR, Supelco) and used as received. Dry solvents were taken from a solvent purification system with activated aluminum oxide columns (Innovative Technology, Inc.).

Flash chromatography was performed using commercial silica gel 230–400 mesh (Silicycle, Inc.).

Solution ¹H, ¹³C {¹H}, ¹⁹F {¹H} NMR spectra were recorded at indicated temperatures on a Bruker Avance 400 MHz spectrometer. All chemical shifts (δ) are reported in ppm and aligned with respect to the residual signal of the corresponding deuterated solvent.¹

Electrospray-ionization (ESI) high-resolution mass spectrometry (HRMS) data were acquired on a Q-ToF Ultima mass spectrometer (Waters) operated in positive mode. Data were processed using Mmass 5.5.0 software. Atmospheric pressure photoionization (APPI) and matrix-assisted laser desorption/ionization (MALDI) HRMS measurements were done on a Linear Trap Quadrupole (LTQ) Orbitrap ETD spectrometer (Thermo Fisher) operated in positive mode.

Relative number (M_n), weight-average (M_w), high average (M_z) molecular weights and polydispersity indexes (PDI as M_w/M_n) of the products were estimated by a Waters Associated gel permeation chromatography (GPC) system equipped with a viscometer as a detector. DMAC + 0.1 wt% LiBr was used as the eluent at the flow rate of 1.0 mL/min and the temperature of 70 °C. A set of monodispersed linear PMMA covering the molecular range of 10³–10⁷ was used as a standard for the molecular weight calibration.

Elemental analyses were performed on an organic elemental analyzer Flash 2000 (Thermo Scientific).

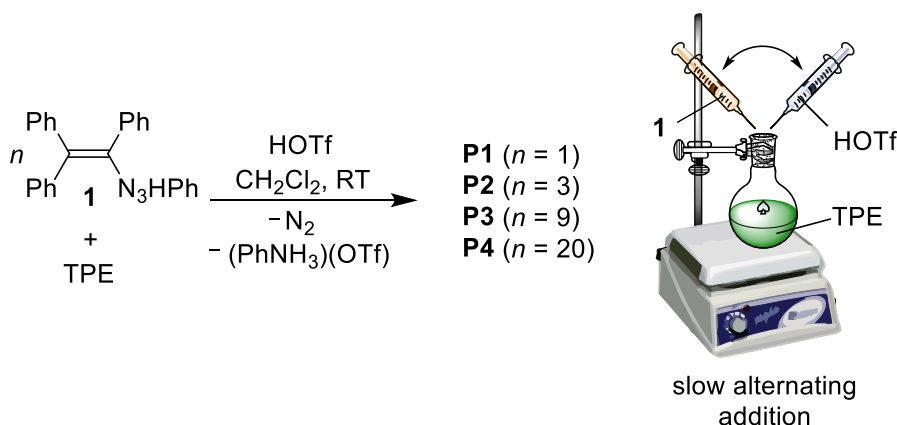
TGA analysis was performed with a Flash 2000 Organic Elemental Analyzer Thermo Scientific.

The DLS measurements were provided on Zetasizer Nano ZS (Malvern) using a QS cuvette 10 mm × 10 mm at 25 °C.

Synthesis of the polymers

Triazene **1** was prepared according to the published procedure.²

General procedure for the synthesis of P1–P4. Tetraphenylethylene (TPE, 1 equiv.) and triazene **1** (1 equiv.) were placed in a screw-cap vial equipped with a stirring bar, dissolved in DCM (0.133 M), and stirred for 10 min at r.t.. Triflic acid (HOTf, 3 equiv.) was added slowly dropwise under vigorous stirring (1200 rpm) using a micropipette with a plastic tip. A color change from yellow to dark red and gas release were observed. The mixture was stirred for 1 h at r.t. (the solution changed color to dark green). Polymerization was achieved through *n*-time dropwise addition of a solution of **1** (1 equiv.) in DCM (0.133 M) followed by the addition of HOTf (3 equiv.) and stirring for 1 h at r.t. after each addition. Subsequently, an excess of dry K₂CO₃ was added, and the dark green mixture was stirred until the color changed to dark red. Then, the suspension was filtered through a pad of cotton wool, and the pad was subsequently washed by portions of DCM. The filtrate was evaporated to a minimum volume, and the product was precipitated with an excess of methanol and centrifuged. The crude product was exposed to 10-min sonication with methanol, washed with diethyl ether/hexane solvent mixture (1:1, v/v) and dried under high vacuum to give powders with a pale yellow to dark orange color.



Scheme S1. Synthesis of the polymers **P1–P4**.

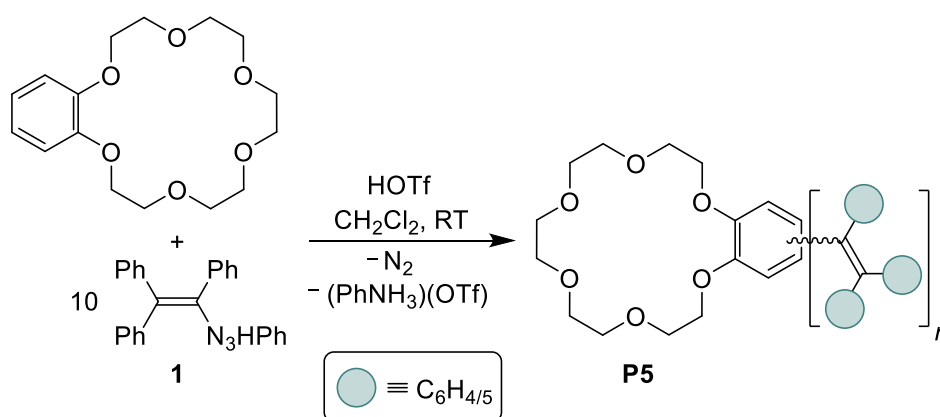
P1 ($n = 1$). Prepared from TPE (44.16 mg, 0.133 mmol, 1 equiv.), **1** (49.88 mg, 0.133 mmol, 1 equiv.) and HOTf (59.85 mg, 0.399 mmol, 35.29 μ L, 3 equiv.). Weight of dry **P1** (pale yellow powder): 14.1 mg. $M_w = 1023$ g/mol, $M_n = 480.2$ g/mol, $M_z = 1596$ g/mol, $PDI = 2.13$. Elem. anal. (%) C, 91.20; H, 3.26; N, 0.00.

P2 ($n = 3$). Prepared from TPE (44.16 mg, 0.133 mmol, 1 equiv.), **1** (149.6 mg, 0.399 mmol, 3 equiv.) and HOTf (179.6 mg, 1.197 mmol, 105.9 μ L, 9 equiv.). Weight of dry **P2** (yellow powder): 48.6 mg. $M_w = 1242$ g/mol, $M_n = 574.2$ g/mol, $M_z = 2183$ g/mol, $PDI = 2.16$. Elem. anal. (%) C, 87.35; H, 4.44; N, 0.00.

P3 ($n = 9$). Prepared from TPE (44.16 mg, 0.133 mmol, 1 equiv.), **1** (450 mg, 1.197 mmol, 9 equiv.) and HOTf (538.7 mg, 3.591 mmol, 317.6 μL , 27 equiv.). Weight of dry **P3** (orange powder): 183.4 mg. $M_w = 2508$ g/mol, $M_n = 923.8$ g/mol, $M_z = 3998$ g/mol, $PDI = 2.72$. Elem. anal. (%) C, 93.01; H, 3.64; N, 0.00.

P4 ($n = 20$). Prepared from TPE (44.16 mg, 0.133 mmol, 1 equiv.), **1** (997.5 mg, 2.660 mmol, 20 equiv.) and HOTf (1197 mg, 7.980 mmol, 705 μL , 60 equiv.). Weight of dry **P4** (dark orange powder): 520.2 mg. $M_w = 3939$ g/mol, $M_n = 1204$ g/mol, $M_z = 9524$ g/mol, $PDI = 3.27$. Elem. anal. (%) C, 94.62; H, 4.02; N, 0.00.

Synthesis of hyperbranched polymer P5. Benzo-18-crown-6 (100.0 mg, 0.320 mmol, 1 equiv.) and triazene **1** (102.2 mg, 0.320 mmol, 1 equiv.) were placed in a screw-cap vial equipped with a stirring bar, dissolved in DCM (0.320 M), and stirred for 10 min at r.t.. HOTf (144.1 mg, 0.960 mmol, 85 μL , 3 equiv.) was added slowly dropwise under vigorous stirring (1200 rpm) using a micropipette with a plastic tip. A color change from yellow to dark red and gas release were observed. The mixture was stirred for 1 h at r.t. (the solution changed color to dark green). Polymerization was achieved through 9-time dropwise addition of first a solution of **1** (102.2 mg, 0.320 mmol, 1 equiv.) in DCM (1.1 M) followed by the addition of HOTf (144.1 mg, 0.960 mmol, 85 μL , 3 equiv.) and stirring for 1 h at r.t. after each addition. Then, the mixture was diluted with DCM to the volume of 100 mL, and the organic phase was washed with water (3 \times 200 mL) until neutral pH, and then with brine. The organic phase was dried over anhydrous Na_2SO_4 and filtered. The filtrate was evaporated to a minimum volume, and the product was precipitated with an excess of methanol and centrifuged. The crude product was exposed to 10-min sonication with methanol, washed with diethyl ether/hexane solvent mixture (1:1, v/v) and dried under high vacuum to give an orange powder.



Scheme S2. Synthesis of the polymer **P5**.

P5. Weight of dry **P5** (orange powder): 565.4 mg. $M_w = 2732$ g/mol, $M_n = 1118$ g/mol, $M_z = 5549$ g/mol, $PDI = 2.44$. Elem. anal. (%) C, 91.45; H, 5.90; N, 0.00.

Mass spectra

Table S1. APPI⁺ MS detection.

| Polymer | Products detected by MS, <i>n</i> |
|-----------|-----------------------------------|
| P1 | up to 7 |
| P2 | up to 9 |
| P3 | up to 11 |
| P4 | up to 11 |
| P5 | up to 8 |

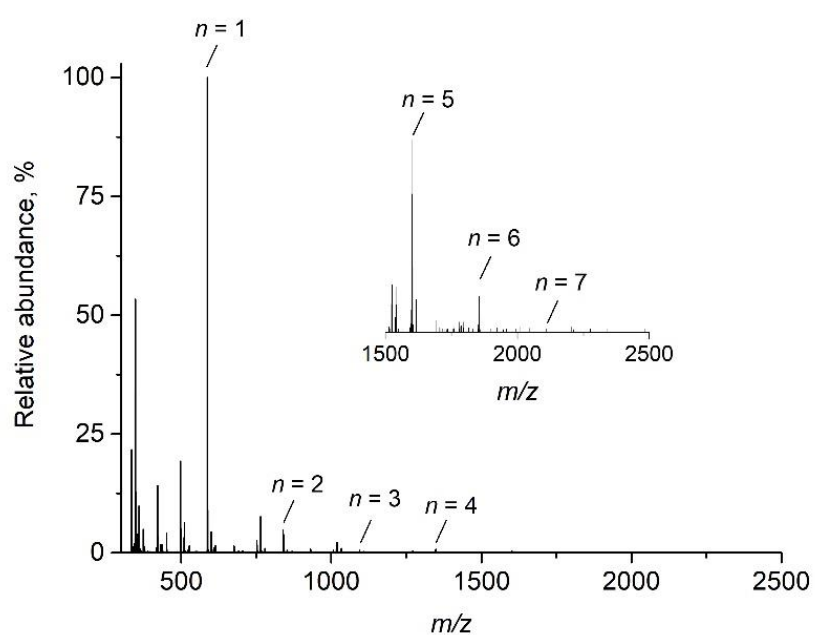


Fig. S1 APPI⁺ HRMS of **P1**.

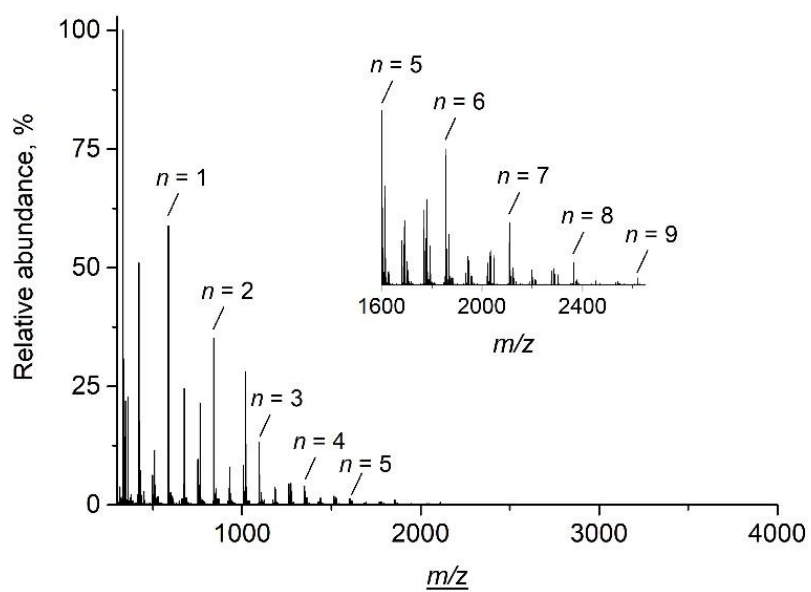


Fig. S2. APPI⁺ HRMS of P2.

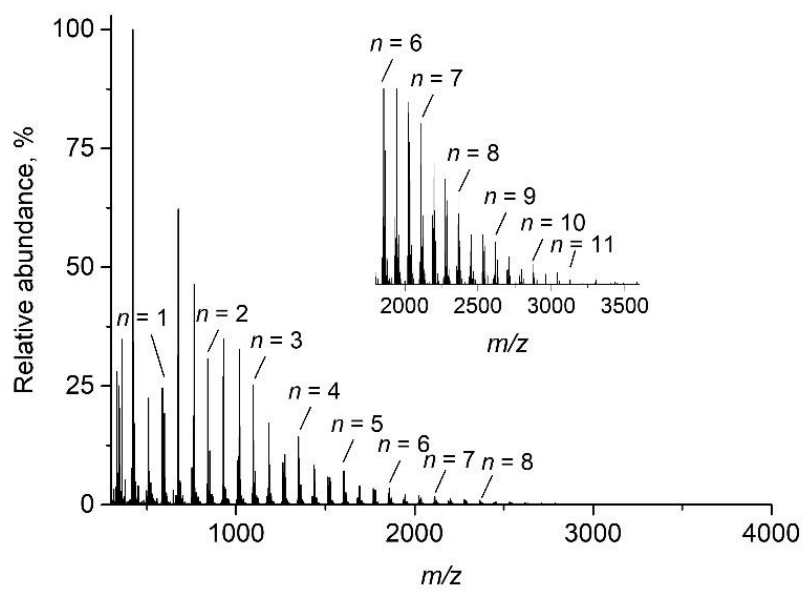


Fig. S3. APPI⁺ HRMS of P3.

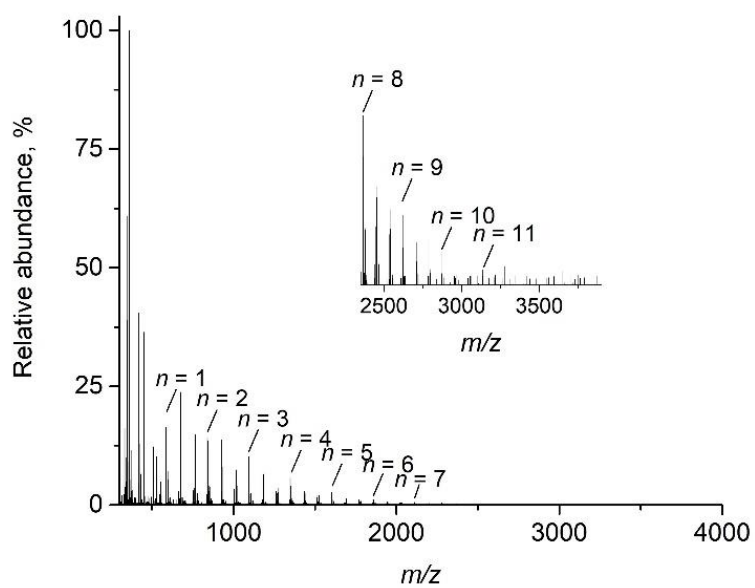


Fig. S4. APPI⁺ HRMS of P4.

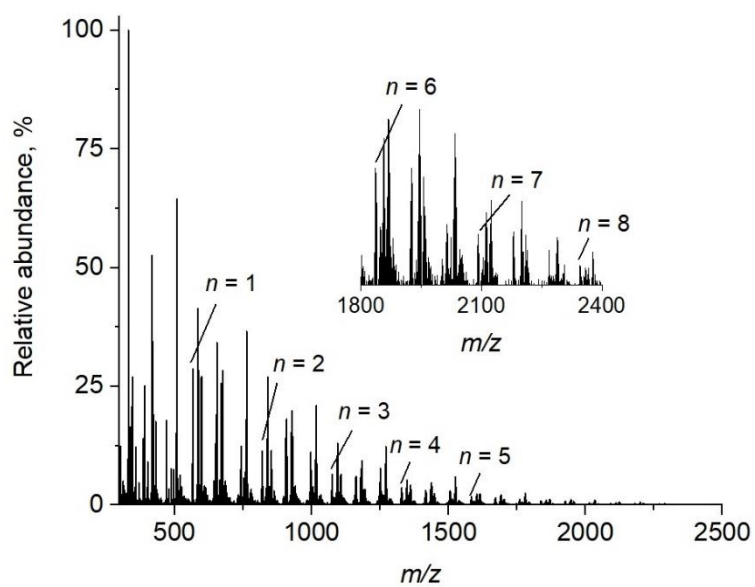


Fig. S5. APPI⁺ HRMS of P5.

Table S2. Summary of the HRMS data for the polymers **P1–P4**.

| <i>n</i> | Formula | Calculated [M] ⁺ , <i>m/z</i> | Found [M] ⁺ , <i>m/z</i> | | | |
|----------|-----------------------------------|--|-------------------------------------|-----------|-----------|-----------|
| | | | P1 | P2 | P3 | P4 |
| 1 | C ₄₆ H ₃₄ | 586.2661 | 586.2713 | 586.2688 | 586.2664 | 586.2631 |
| 2 | C ₆₆ H ₄₈ | 840.3756 | 840.3810 | 840.3808 | 840.3771 | 840.3717 |
| 3 | C ₈₆ H ₆₂ | 1094.4852 | 1094.4902 | 1094.4900 | 1094.4868 | 1094.4802 |
| 4 | C ₁₀₆ H ₇₆ | 1349.5981 | 1349.6011 | 1349.6026 | 1349.6006 | 1349.5938 |
| 5 | C ₁₂₆ H ₉₀ | 1603.7076 | 1603.7122 | 1603.7117 | 1603.7111 | 1603.7025 |
| 6 | C ₁₄₆ H ₁₀₄ | 1857.8172 | 1857.8274 | 1857.8176 | 1857.8206 | 1857.8104 |
| 7 | C ₁₆₆ H ₁₁₈ | 2111.9267 | 2111.2572 | 2111.9277 | 2111.9297 | 2111.9166 |
| 8 | C ₁₈₆ H ₁₃₂ | 2367.0396 | – | 2367.0550 | 2367.0436 | 2367.0294 |
| 9 | C ₂₀₆ H ₁₄₆ | 2621.1492 | – | 2621.1434 | 2621.1504 | 2621.1481 |
| 10 | C ₂₂₆ H ₁₆₀ | 2875.2587 | – | – | 2875.2715 | 2875.2658 |
| 11 | C ₂₄₆ H ₁₇₄ | 3129.3683 | – | – | 3129.4014 | 3129.3880 |

Table S3. Summary of the HRMS data for polymer **P5**.

| <i>n</i> | Formula | Calculated [M] ⁺ , <i>m/z</i> | Found [M] ⁺ , <i>m/z</i> |
|----------|--|--|-------------------------------------|
| 1 | C ₃₆ H ₃₈ O ₆ | 566.2668 | 566.2675 |
| 2 | C ₅₆ H ₅₂ O ₆ | 820.3764 | 820.3769 |
| 3 | C ₇₆ H ₆₆ O ₆ | 1074.4859 | 1074.4863 |
| 4 | C ₉₆ H ₈₀ O ₆ | 1328.5955 | 1328.5938 |
| 5 | C ₁₁₆ H ₉₄ O ₆ | 1583.7084 | 1583.7107 |
| 6 | C ₁₃₆ H ₁₀₈ O ₆ | 1836.8146 | 1836.8144 |
| 7 | C ₁₅₆ H ₁₂₂ O ₆ | 2090.9241 | 2090.9233 |
| 8 | C ₁₇₆ H ₁₃₆ O ₆ | 2345.0337 | 2345.0370 |

NMR spectra

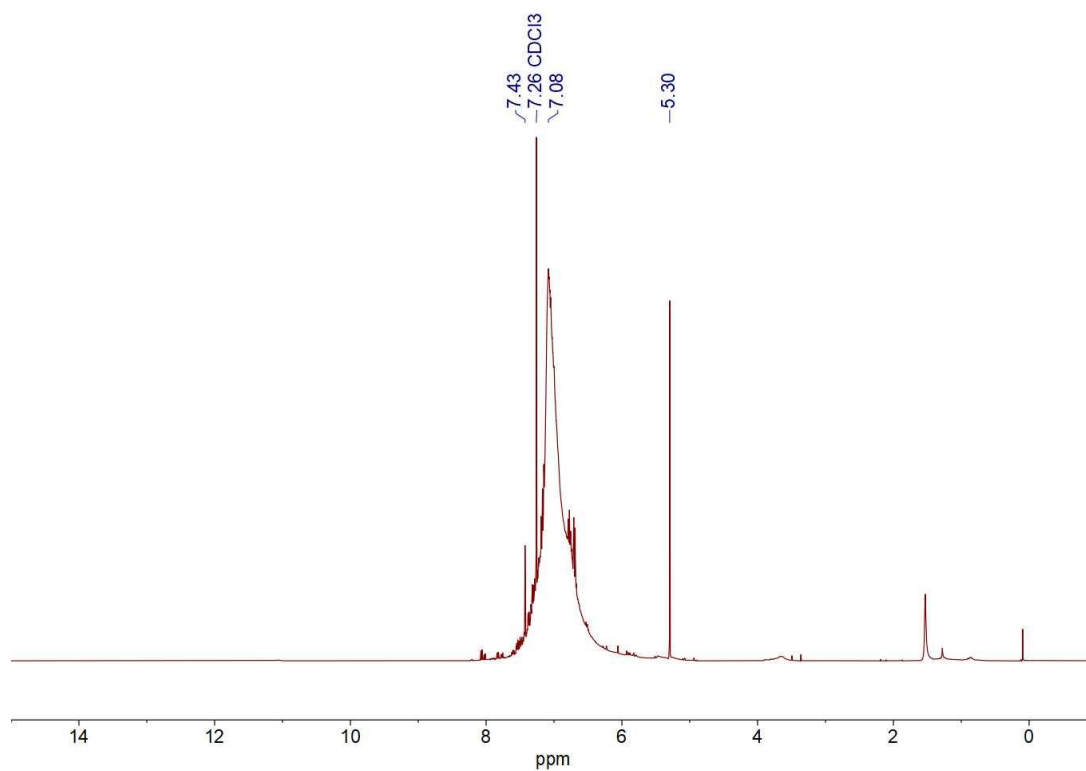


Fig. S6. ¹H NMR (400 MHz, CDCl₃, 298 K) spectrum of **P4**.

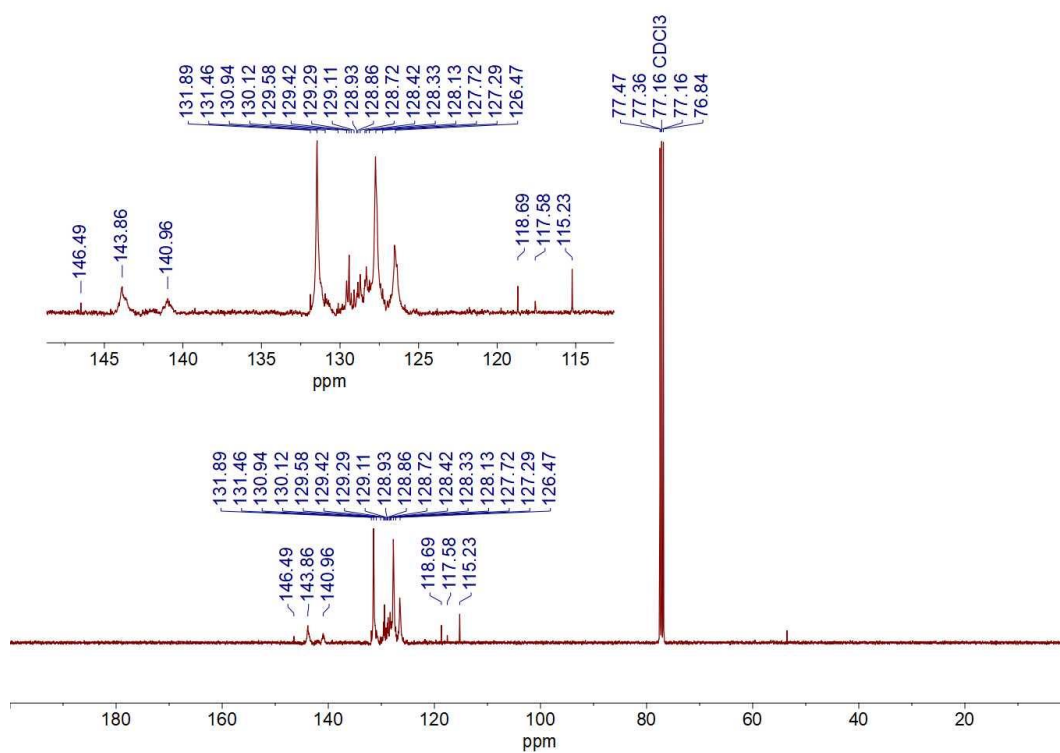


Fig. S7. ¹³C NMR (101 MHz, CD₂Cl₂, 298 K) spectrum of **P4**. The spectrum resembles that of TPE.³

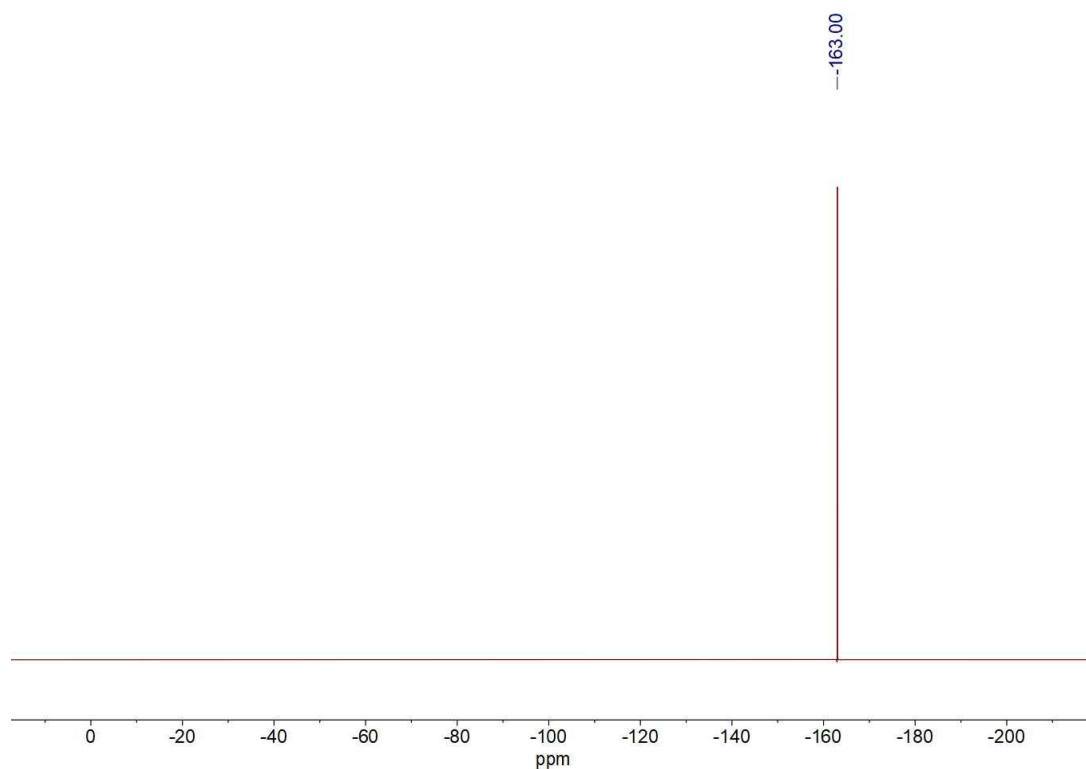


Fig. S8. ^{19}F NMR (376 MHz, CDCl_3 , 298 K) spectrum of **P4** with hexafluorobenzene as a standard ($\delta_{\text{C}_6\text{F}_6} = -163.0$ ppm). The absence of other peaks than that of C_6F_6 confirms that there are no $-\text{CF}_3$ groups in **P4** ($\delta_{\text{F}}(-\text{SO}_3\text{CF}_3)$ is -50 to -80 ppm^{4,5}).

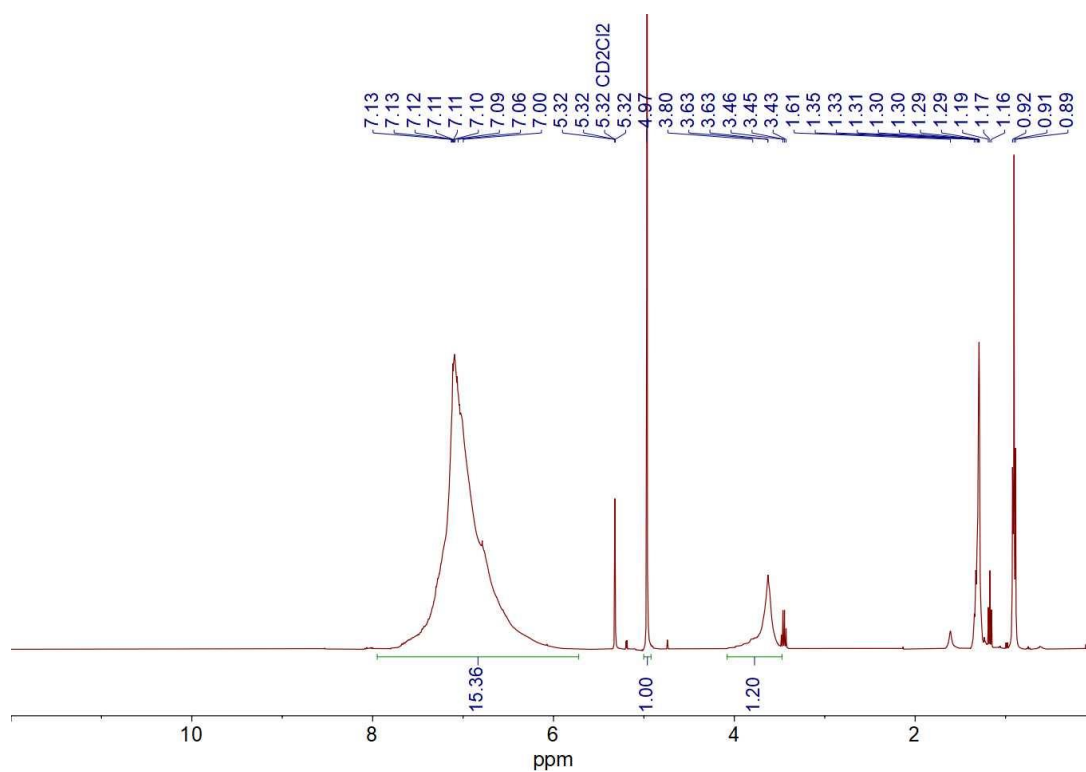


Fig. S9. ^1H NMR (400 MHz, CDCl_3 , 298 K) spectrum of **P5**. The signal at 4.76 ppm belongs to the internal standard CH_2Br_2 .

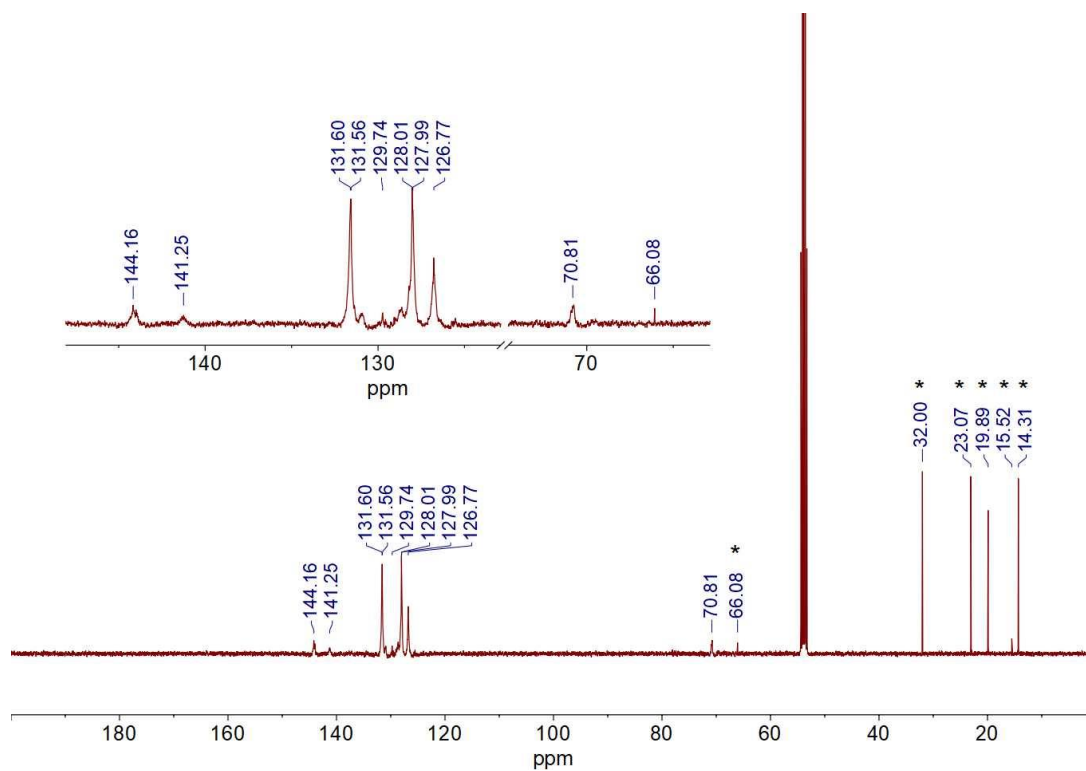


Fig. S10. ^{13}C NMR (101 MHz, CD_2Cl_2 , 298 K) spectrum of **P5**. The signals marked by asterisks belong to internal standard CH_2Br_2 , and the solvents (Et_2O and *n*-hexane) which could not be removed after synthesis by drying under high vacuum.

Thermogravimetric analyses of the polymers

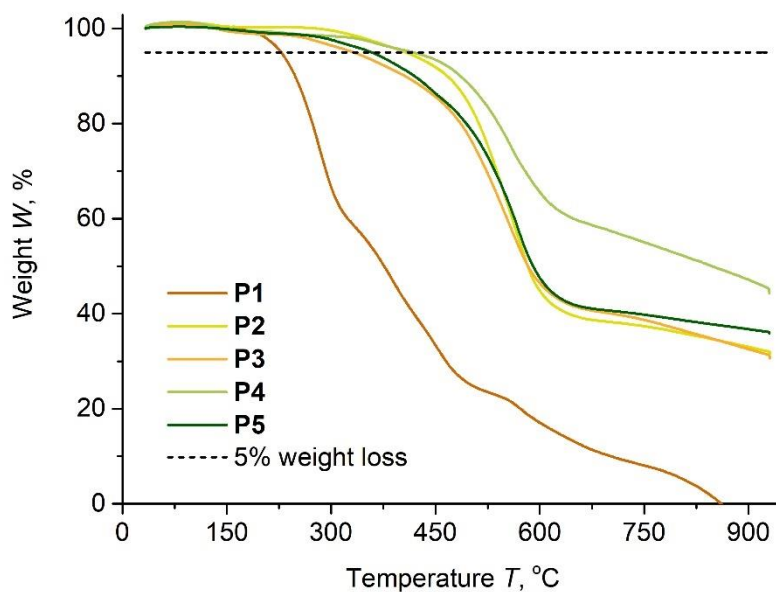


Fig. S11. TGA thermograms of polymers **P1–P5**. Program: N₂, 30 °C to 900 °C with step 10 °C/min, flow rate: 20 mL/min.

Table S4. Thermogravimetric data.

| Compound | Degradation temperature (T_d) at 5% weight loss, °C |
|---|---|
| P1 | 228 (melting point is 234 – 236 °C) |
| P2 | 332 |
| P3 | 407 |
| P4 | 420 |
| P5 | 358 |
| Linear poly(triphenylethene) ⁶ | 402 |
| Linear poly(tetraphenylethene) ⁶ | 400 |

Photophysical properties

Photophysical measurements for TPE and for the polymers **P1–P5** were performed on aerated optically diluted ($A < 0.1$) solutions of spectrophotometric grade THF placed in a Quartz Suprasil cuvette (QS, 10×10 mm). The samples were prepared according to the following procedure: ≈1.1 mg of the polymer was weighted, placed in a vial, dissolved in 3 mL of THF and then the concentrated solution was diluted by taking a 50 μL aliquot of it and addition of 4950 μL of THF. Absorption spectra were measured on a Cary 60 spectrophotometer (Agilent Technologies). Emission spectra were recorded on a Cary Eclipse fluorescence spectrometer (Varian).

Photoluminescence lifetimes (τ) were measured on a time-correlated single photon counting Edinburgh LifeSpec II spectrometer using an Edinburgh Picosecond pulsed diode lasers ($\lambda_{exc} = 405$ nm) as excitation sources. The fitting of the emission decays was performed by using Fluoracle software. The quality of the fitting was evaluated via the analysis of the χ^2 parameter and of the residual distribution.

Solid state quantum yields (Φ_{solid}) were measured with an integrating sphere module of the Edinburgh FS5, and quantum yield values were calculated with Fluoracle software.

Photoluminescence quantum yields of the polymers **P1**, **P4** and **P5** in aerated THF solutions were measured relative to quinine sulphate (QS) in 0.5 M H_2SO_4 . Following the standard procedure for determination of quantum yields,⁷ absorption and emission ($\lambda_{exc} = 366$ nm) spectra were recorded for solutions of QS, **P1**, and **P4** with a gradual change of concentration. Then, a linear approximation of integral emission intensity vs absorbance was plotted, and a slope k was determined. The relative quantum yield of the polymers Φ_X was then calculated using the following equation:

$$\Phi_X = \Phi_{ST} \left(\frac{k_X}{k_{ST}} \right) \left(\frac{n_X^2}{n_{ST}^2} \right),$$

where Φ_{ST} is absolute quantum yield of the standard, $\Phi_{QS} = 0.546$ ($\lambda_{exc} = 366$ nm),⁸ k_X and k_{ST} are slopes for the linear approximation for the sample and the standard, respectively, $\frac{n_X^2}{n_{ST}^2}$ is refractive indexes ratio for sample solvent ($n_{THF} = 1.404$)⁹ and the standard ($n_{0.5 M H_2SO_4} = 1.346$)¹⁰ at 25 °C.

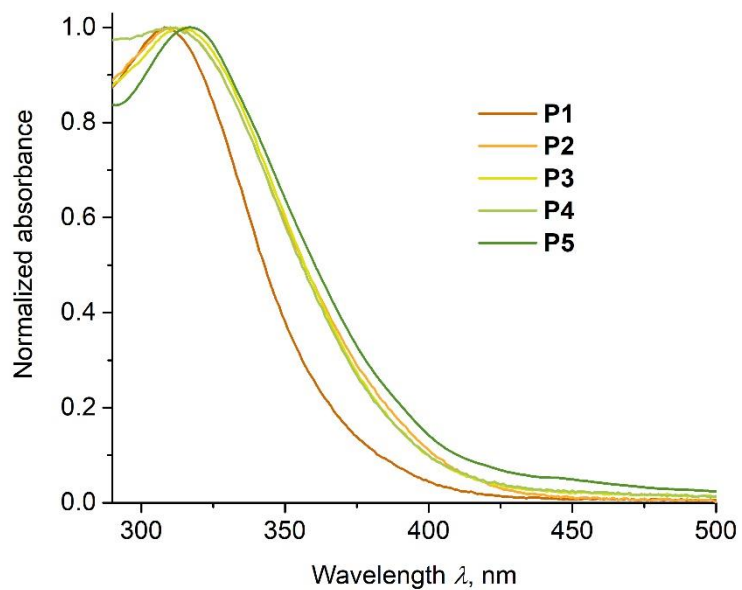
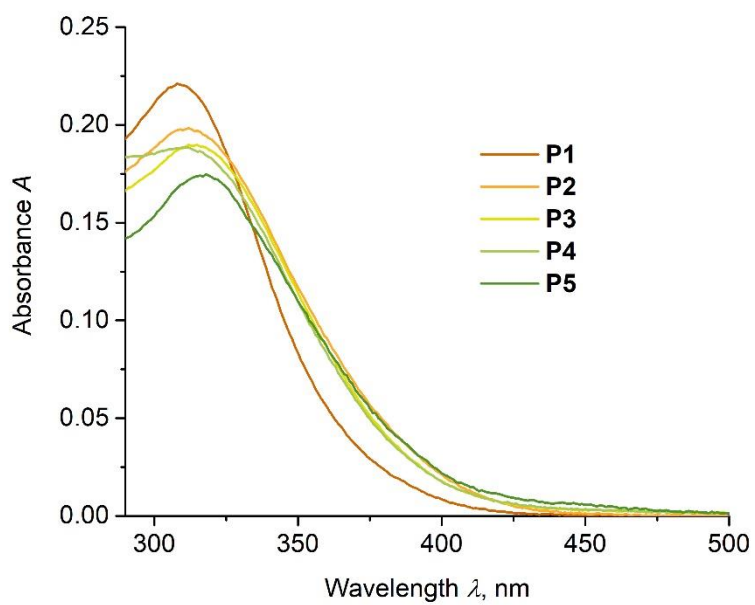


Fig. S12. Absolute (top) and normalized (bottom) UV-Vis spectra of the polymers **P1–P5** in THF.

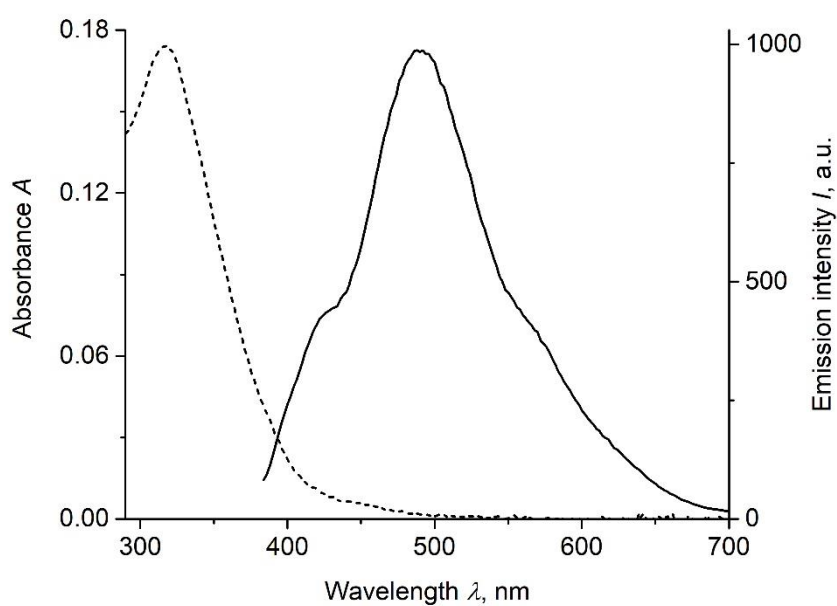


Fig. S13. UV-Vis (dashed) and photoluminescence (solid) spectra of polymer **P5** in THF ($\lambda_{exc} = 365$ nm, $[P5] = 0.4$ $\mu\text{g/mL}$).

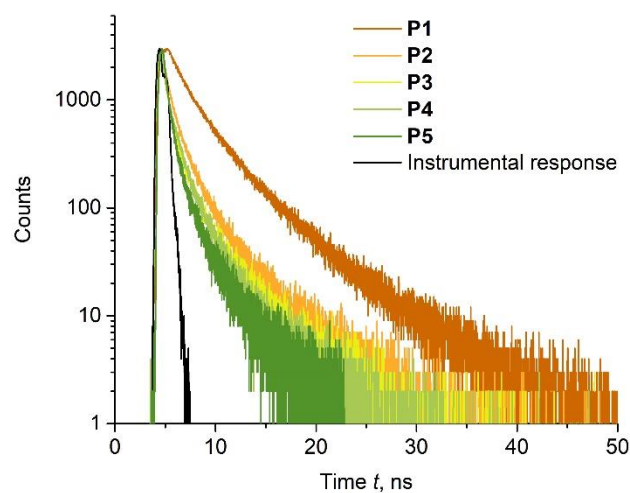


Fig. S14. Photoluminescence decay curves at 500 nm for the polymers **P1–P5** recorded by time-correlated single photon counting ($\lambda_{exc} = 405$ nm).

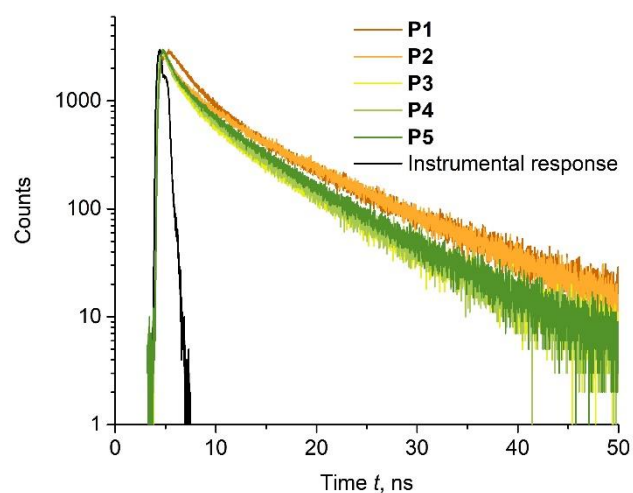


Fig. S15. Photoluminescence decay curves at 600 nm for the polymers **P1–P5** recorded by time-correlated single photon counting ($\lambda_{exc} = 405$ nm).

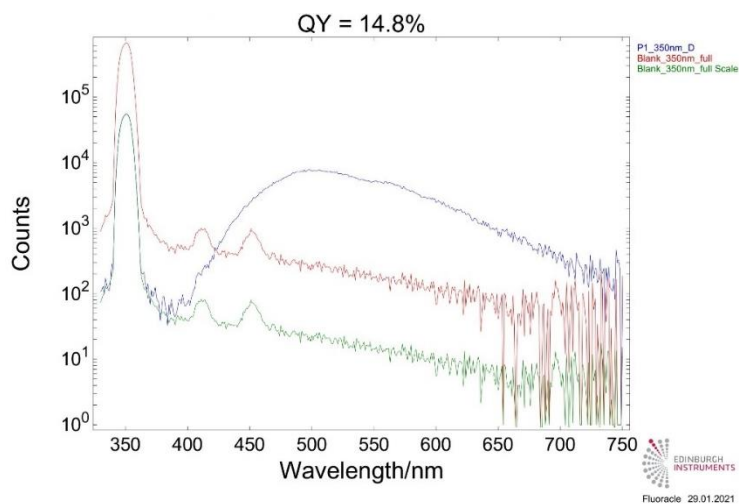


Fig. S16. Solid state quantum yield calculation of **P1** ($\lambda_{exc} = 350$ nm).

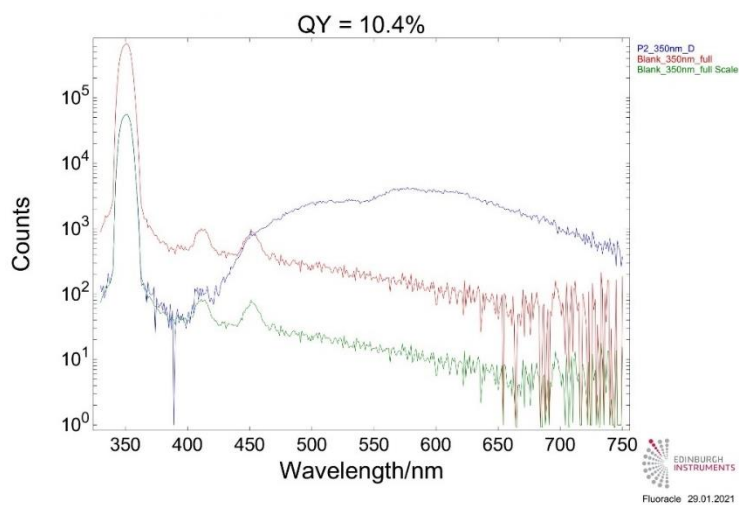


Fig. S17. Solid state quantum yield calculation of **P2** ($\lambda_{exc} = 350$ nm).

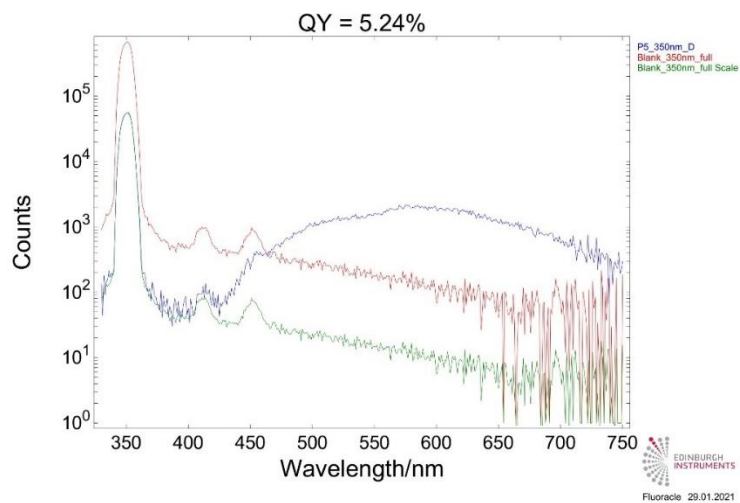


Fig. S18. Solid state quantum yield calculation of **P3** ($\lambda_{exc} = 350$ nm).

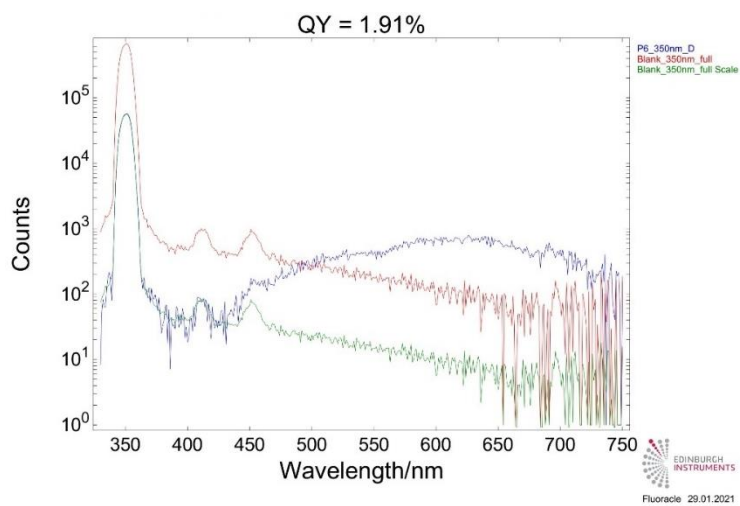


Fig. S19. Solid state quantum yield calculation of **P4** ($\lambda_{exc} = 350$ nm).

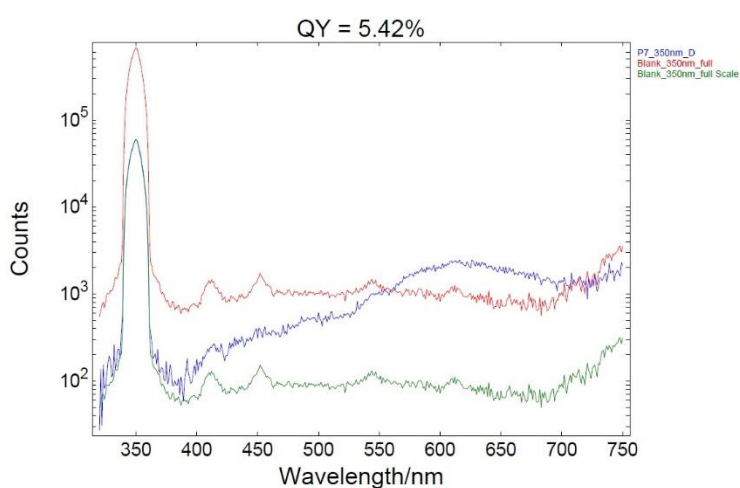


Fig. S20. Solid state quantum yield calculation of **P5** ($\lambda_{exc} = 350$ nm).

Table S5. Optical properties and photoluminescence quantum yields of the compounds.

| Compound | λ_{abs} , nm | λ_{em}^{sol} , nm | λ_{em}^{solid} , nm | Φ_{solid} , % | Φ_{sol}^a , % |
|-----------|----------------------|---------------------------|-----------------------------|--------------------|--------------------|
| TPE | 309 | 414 | 443 | 23.0 ¹¹ | – |
| P1 | 308 | 499 | 488 | 14.8 | 0.05 |
| P2 | 312 | 498 | 505, 575sh | 10.4 | – |
| P3 | 315 | 494 | 503, 574 | 5.2 | – |
| P4 | 316 | 502 | 515, 579 | 1.9 | 0.46 |
| P5 | 318 | 425sh, 490, 575sh | 500sh, 600 | 5.4 | 0.32 |

^a Photoluminescence quantum yields in solution were measured relatively to quinine sulphate in 0.5 M H₂SO₄, λ_{ex} = 366 nm, 298 K.

Table S6. Photoluminescence lifetimes of the polymers.

| Compound | τ^a , ns (λ_{em} = 500 nm) | τ , ns (λ_{em} = 600 nm) |
|-----------|--|--|
| P1 | 1.23 (24.3); 4.03 (76.7) | 1.92 (29.1); 8.49 (70.9) |
| P2 | 1.28 (28.0); 4.11 (72.0) | 1.27 (15.0); 6.18 (85.0) |
| P3 | 794 ps (60.4); 2.93 (39.6) | 1.11 (18.2); 5.57 (81.8) |
| P4 | 753 ps (45.9); 2.83 (54.1) | 1.27 (15.9); 5.68 (84.1) |
| P5 | 0.49 (50.0); 1.85 (50.0) | 1.00 (16.8); 5.65 (83.3) |

^a The relative contributions of the components of the double exponential decay are given in parenthesis.

Aggregation-induced emission of the polymers

In a 15 mL screw-cap vial, 2.5 mg of the respective polymer was dissolved in a volume of THF, dioxane, or DMF according to indicated antisolvent (water, hexane or MeOH) fraction f , *i.e.* 10 mL – 0%, ..., 1 mL – 90%. A magnetic stirring bar was placed in the vial and the corresponding volume of antisolvent was added slowly (dropwise) under rapid stirring (1200 rpm), *i.e.* 1 mL – 10%, ..., 9 mL – 90%. Emission spectra were recorded immediately after the addition of antisolvent.

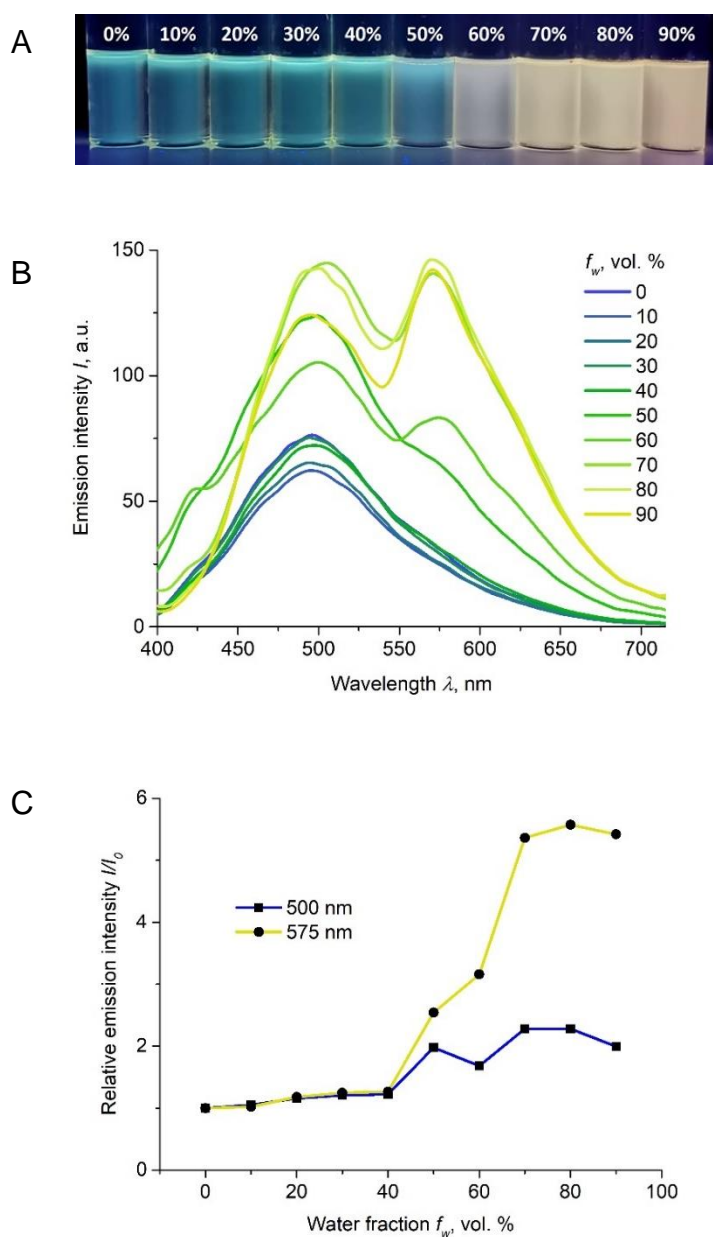


Fig. S21. (A) Photo images of **P3** in THF/water mixtures (f_w is indicated). (B) Emission spectra and (C) emission enhancement of **P3** in THF/water mixtures ($\lambda_{exc} = 365$ nm).

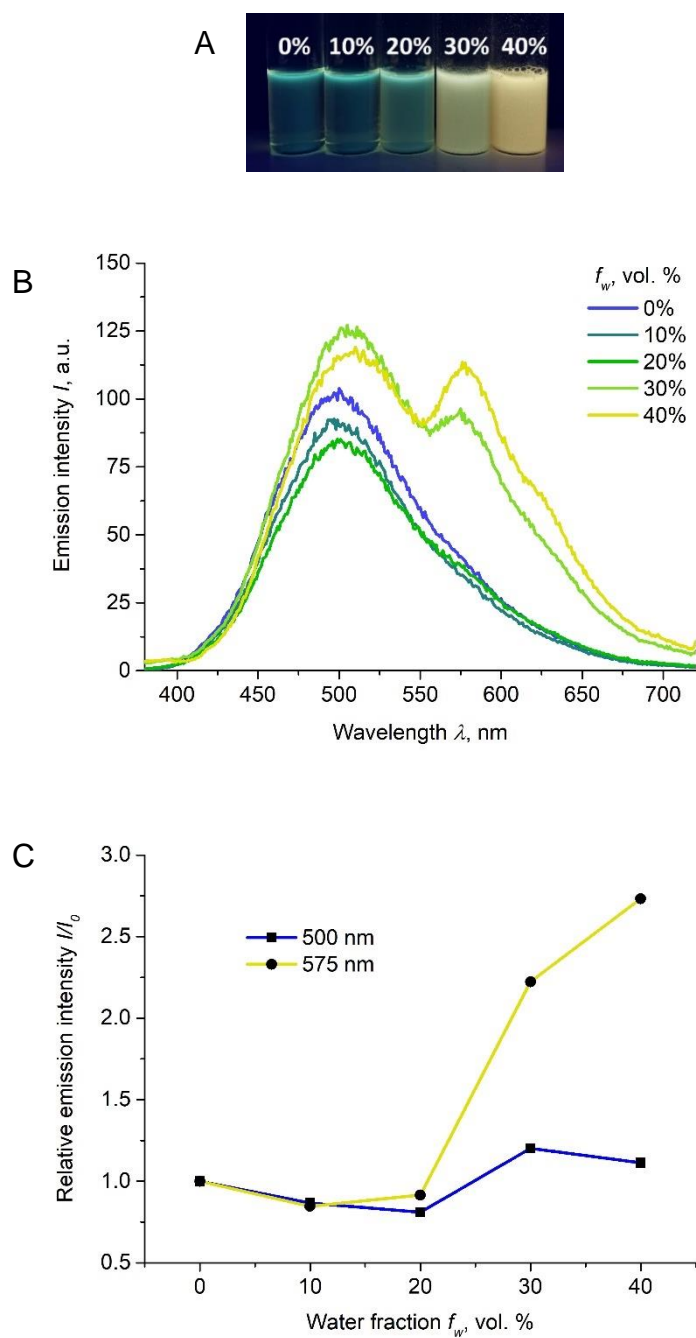


Fig. S22. (A) Photo images of **P4** in dioxane/water mixtures (f_w is indicated). (B) Emission spectra and (C) emission enhancement of **P4** in dioxane/water mixtures ($\lambda_{exc} = 365$ nm).

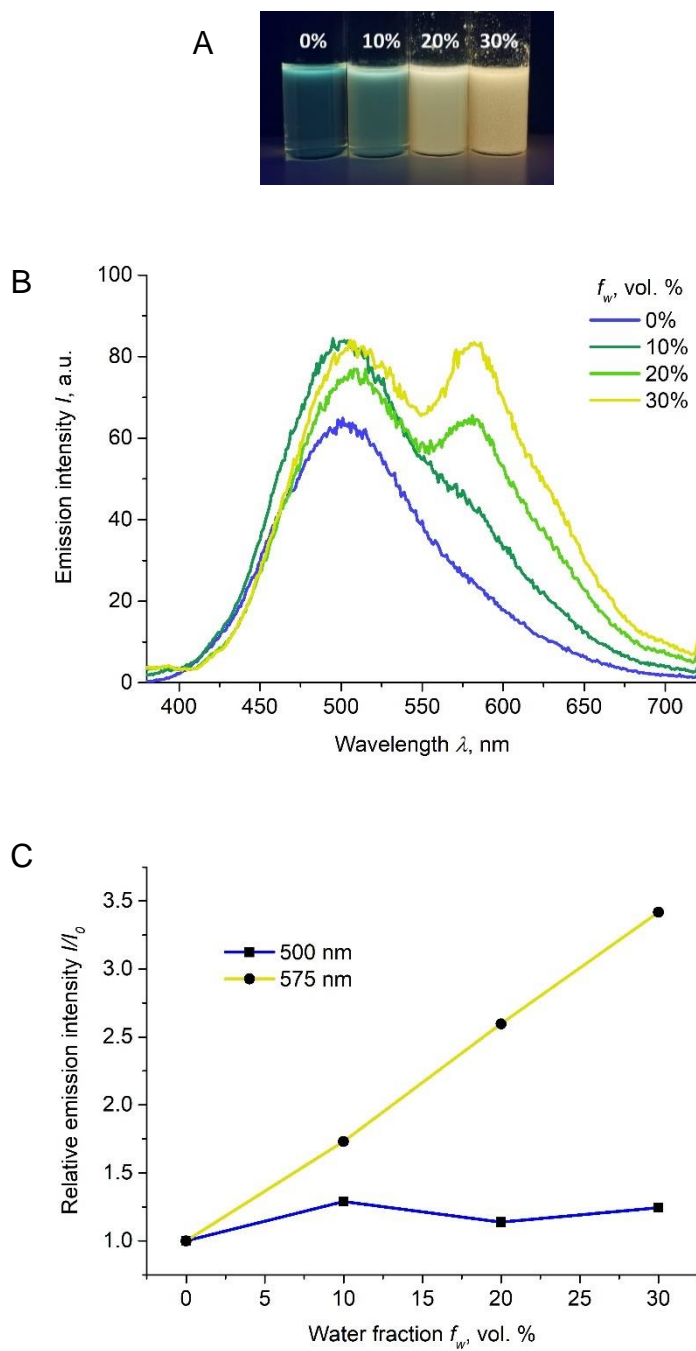


Fig. S23. (A) Photo images of **P4** in DMF/water mixtures (f_w is indicated). (B) Emission spectra and (C) emission enhancement of **P4** in DMF/water mixtures ($\lambda_{exc} = 365$ nm).

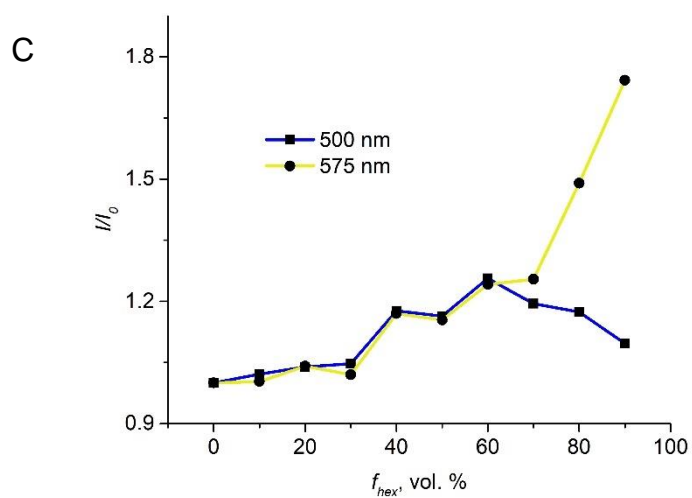
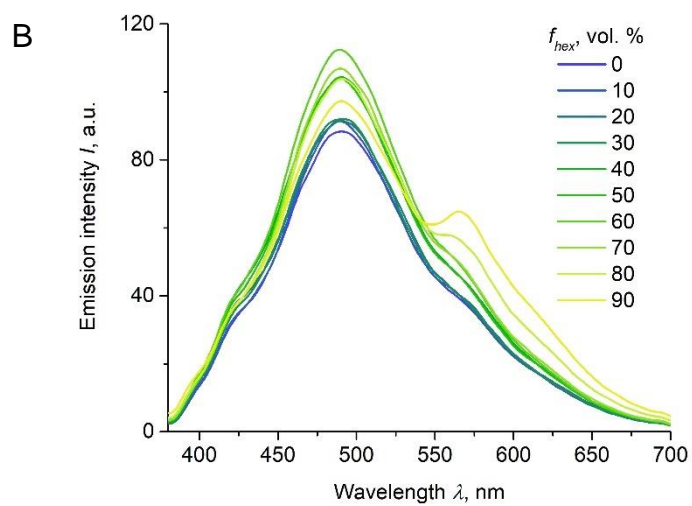
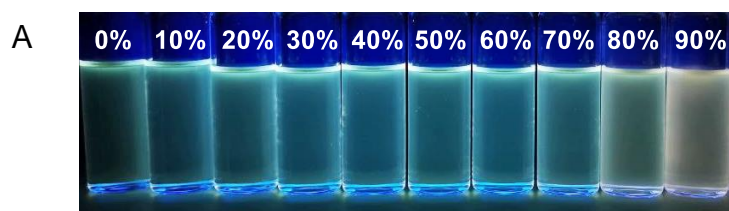


Fig. S24. (A) Photo images of **P5** in THF/hexane mixtures (f_{hex} is indicated). (B) Emission spectra and (C) emission enhancement of **P5** in THF/hexane mixtures ($\lambda_{exc} = 365$ nm).

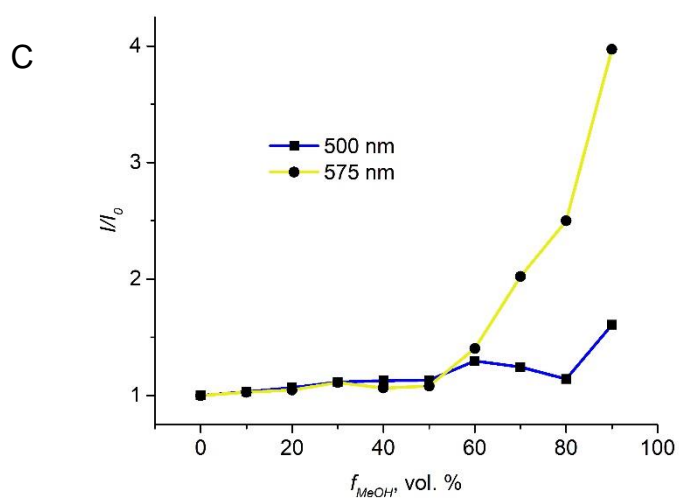
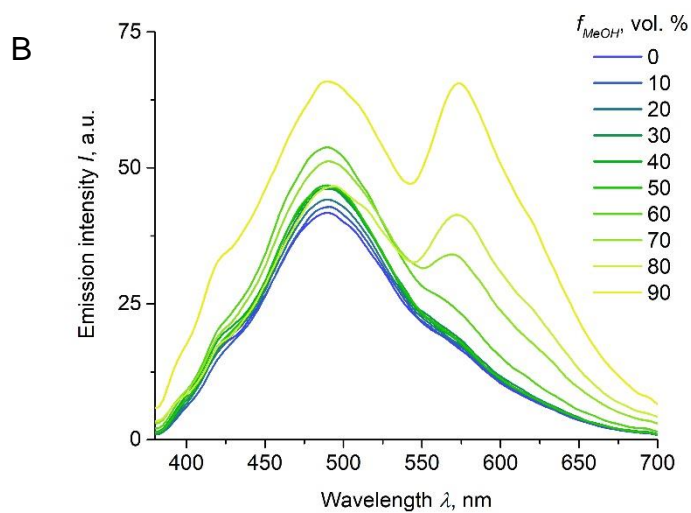
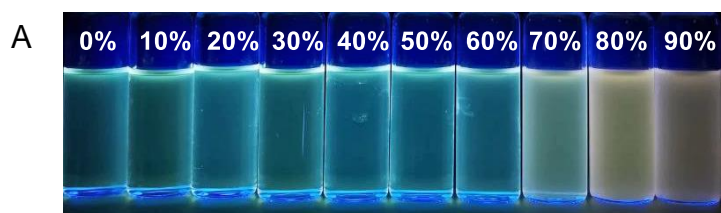


Fig. S25. (A) Photo images of **P5** in THF/MeOH mixtures (f_{MeOH} is indicated). (B) Emission spectra and (C) emission enhancement of **P5** in THF/MeOH mixtures ($\lambda_{exc} = 365$ nm).

Sensing of the cations

A photoluminescence titration was carried out by adding aliquots (μL) of an aqueous KCl solution (2 mg/mL) to a suspension of **P5** (2.5 mg) in THF–water (10 mL, $v/v = 1:1$). A concentration of $[\text{MCl}] = 0.3 \text{ mM}$ was chosen to study the photoluminescence response of **P5** for different alkali metal chlorides (Li, Na, Rb, or Cs) and potassium salts with various anions (F, Br, I, OAc, BF_4 , PF_6 , NO_3). For that, the volume equivalent to a final concentration of 0.3 mM of aqueous solutions of salts (2 mg/mL) was added to a suspension of **P5** (2.5 mg) in THF–water (10 mL, $v/v = 1:1$) under rapid stirring (1200 rpm).

Solid state sensing was carried out by grinding solid **P5** ($\sim 50 \text{ mg}$) with KCl ($\sim 50 \text{ mg}$) in an agate mortar. The photoluminescence response was measured by placing solid **P5** (not ground, ground, ground with KCl) on the walls of a QS cuvette (10 mm \times 10 mm).

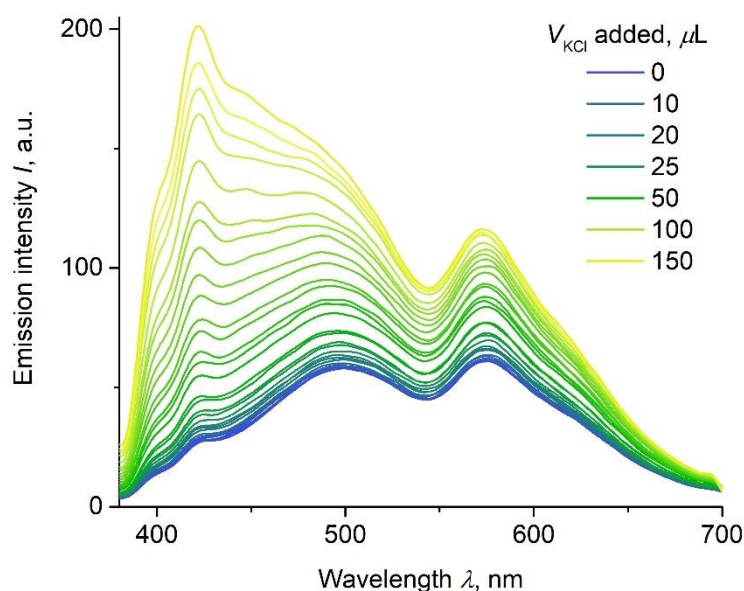


Fig. S26. PL spectra ($\lambda_{exc} = 365 \text{ nm}$) of **P5** (2.5 mg) in THF–water (10 mL, $v/v = 1:1$) after addition of increasing amounts of aqueous KCl.

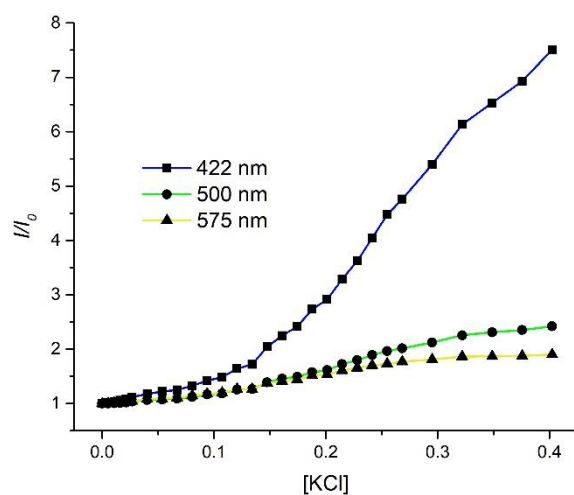


Fig. S27. Luminescence change vs [KCl] at different emission wavelengths. **P5** in THF-water ($v/v = 1:1$). I_0 = intensity at [KCl] = 0 mM. $\lambda_{exc} = 365$ nm.

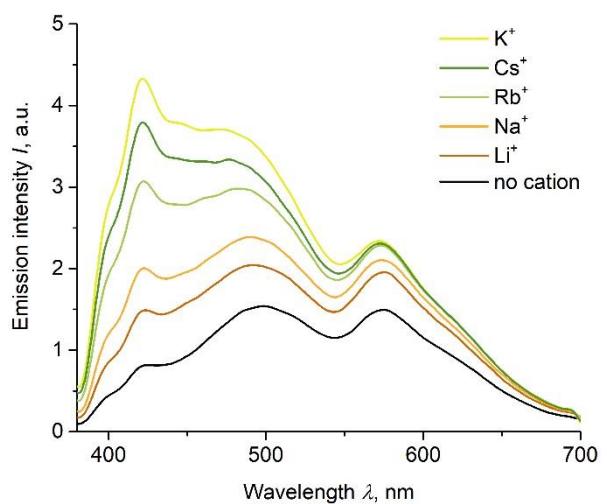


Fig. S28. Emission spectra ($\lambda_{exc} = 365$ nm) and photographs of **P5** in THF-water ($v/v = 1:1$) with and without different MCl salts ([MCl] = 0.3 mM).

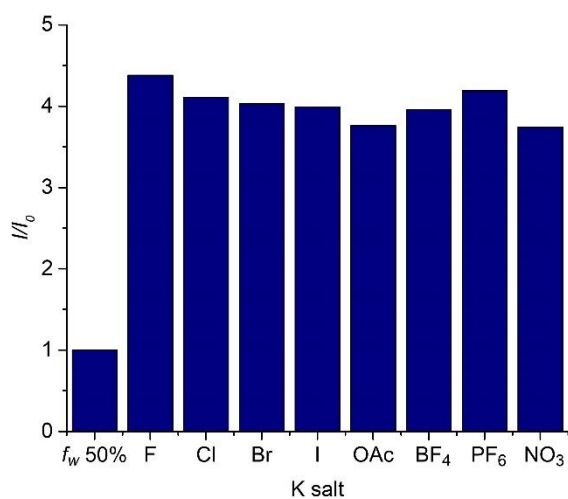
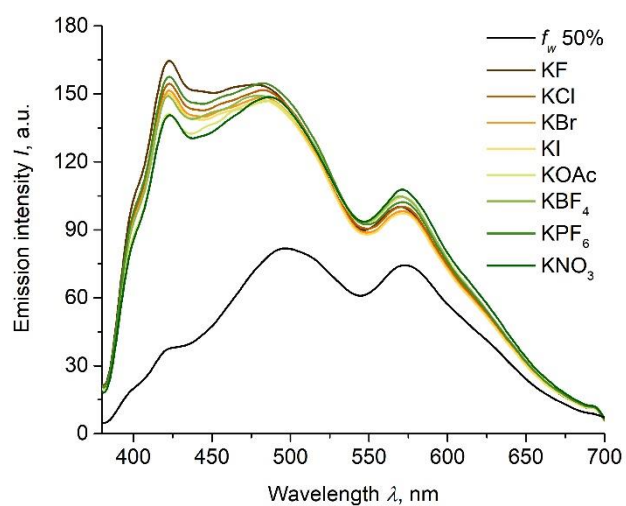


Fig. S29. Emission spectra ($\lambda_{exc} = 365$ nm, top) and emission change at 423 nm (bottom) for **P5** in THF–water ($v/v = 1:1$) with and without different potassium salts ($[KX] = 0.3$ mM).

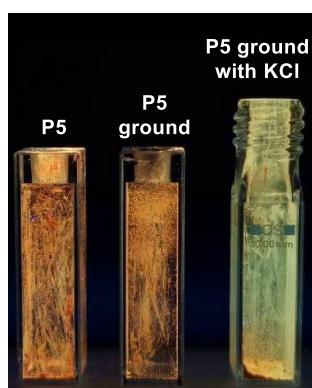
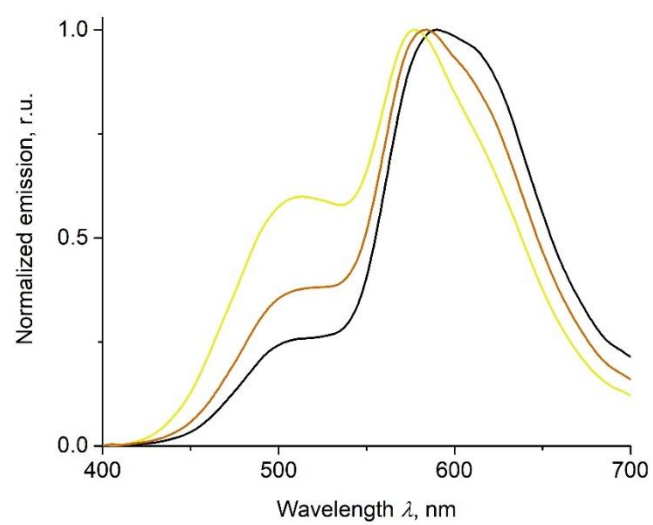


Fig. S30. Normalized emission spectra and photographs (under UV lamp with $\lambda_{exc} = 366$ nm) of **P5** not ground, ground, and ground with KCl.

CIE chromaticity diagrams

The CIE chromaticity diagrams were created using the software ColorCalculator v. 7.77. In the software, the emission spectra were converted to the chromaticity coordinates (x,y) and placed in the CIE 1931 2° color space.

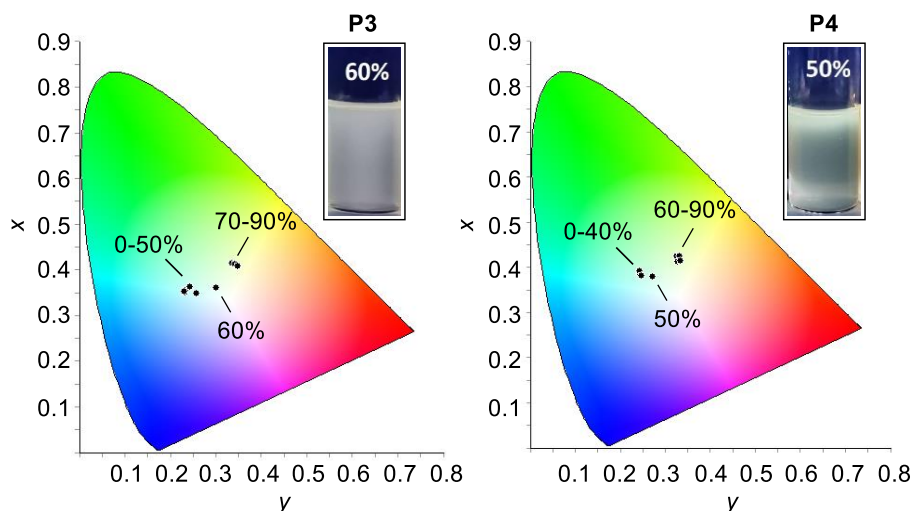


Fig. S31. CIE 1931 2° chromaticity diagrams of **P3** (left) and **P4** (right) in THF/water mixtures (f_w is indicated) and comparison of photo images of **P3** ($f_w = 60\%$) and **P4** ($f_w = 50\%$) under UV light ($\lambda_{exc} = 365$ nm).

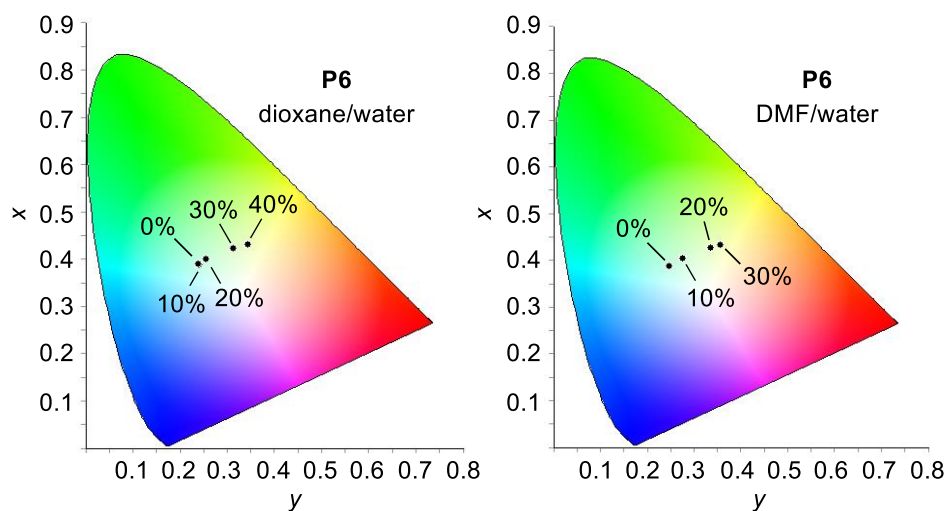


Fig. S32. CIE 1931 2° chromaticity diagrams of **P4** in dioxane/water and DMF/water mixtures (f_w is indicated).

DLS measurements

A solution of **P5** in THF-water (1:1, v/v) was freshly prepared according to the experiment described on Page S19 and diluted 25 times (final concentration: **[P5]** = 10 µg/mL). The solution was placed in a QS cuvette (10 mm × 10 mm), and the intensity-based particle size distribution was determined with three consequent measurements to follow the dynamics of the system. We were able to detect nanoparticles with a size of ~ 1.3 nm and ~ 220 nm. The former are stable within the timeframe of the measurements, whereas the latter seem to undergo further aggregation (increase of size with time).

The software report is provided below.

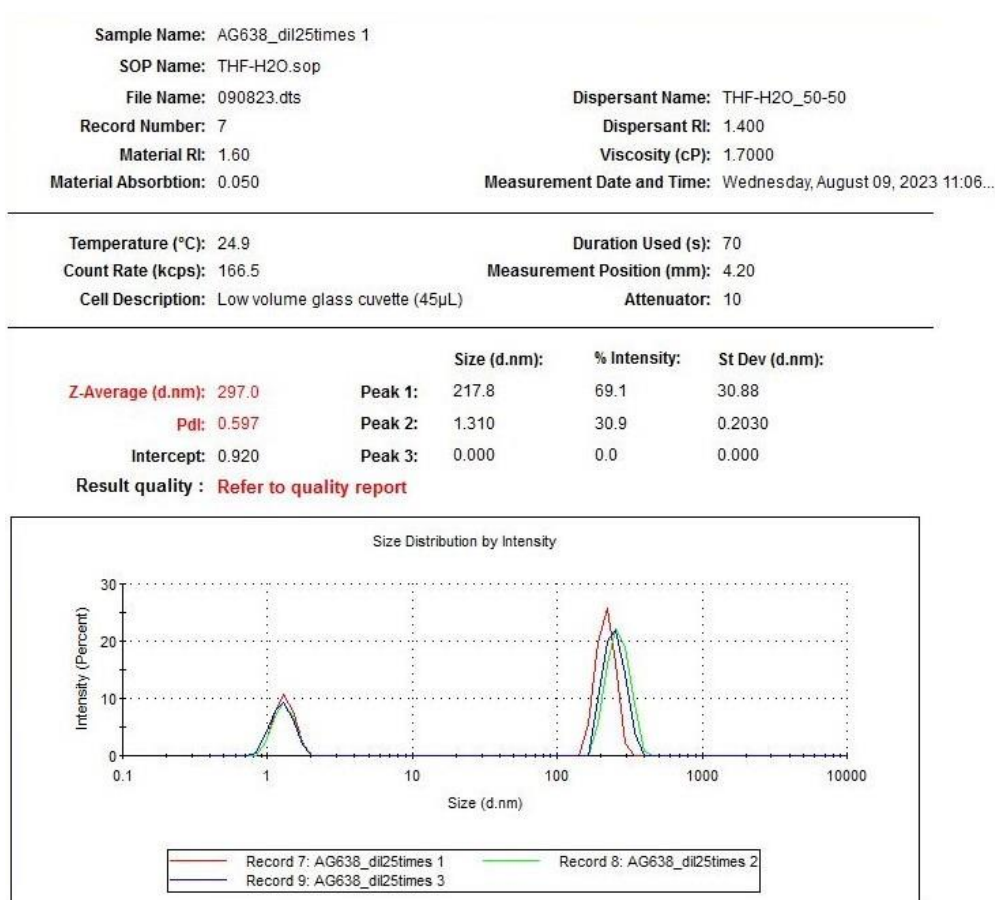


Fig. S33. Summary of the DLS measurements with **P5**.

Optimization of the reaction conditions

The conditions for the polymerization were optimized by examination of the effects of different parameters including acid strength, addition sequence, concentration of TPE, of acid, and of triazene **1**, the addition method, and the technique used. The workup procedure was selected based on the solubility of the polymers.

HRMS with matrix-assisted laser desorption ionization (MALDI) and atmospheric pressure photoionization (APPI) in positive mode were used to observe how the aforementioned parameters influence the polymerization by the detection of the products with low n (Scheme S1). The results are summarized in Table S7.

Table S7. Optimization of the reaction conditions.

| Entry | Effect | TPE ^a , equiv. | 1 , equiv. | HOTf, equiv. | TFA, equiv. | Products, n | | | | | |
|-------|---|------------------------------|-------------------|-----------------|----------------|---------------|---|---|---|---|---|
| | | | | | | 1 | 2 | 3 | 4 | 5 | 6 |
| 1 | Acid strength ^b | 1 | 1 | 5 | – | + | + | + | + | – | – |
| 2 | | 1 | 1 | – | 5 | – | – | – | – | – | – |
| 3 | Addition sequence ^b | 1 | 1 | 5 (last) | – | + | + | + | + | – | – |
| 4 | | 1 | 1 (last) | 5 | – | + | + | – | – | – | – |
| 5 | TPE concentration ^b | 5 | 1 | 5 | – | + | + | – | – | – | – |
| 6 | | 0.5 | 1 | 5 | – | + | + | + | + | – | – |
| 7 | HOTf concentration ^b | 1 | 1 | 3 | – | + | + | + | + | – | – |
| 8 | | 1 | 1 | 1.1 | – | + | + | + | + | – | – |
| 9 | Addition method I ^b | 1 | 5 | 5.5 | – | – | – | – | – | – | – |
| 10 | | 1 | 10 | 11 | – | – | – | – | – | – | – |
| 11 | Addition method II ^b | 1 | 5 | 5.5 | – | + | + | + | + | + | – |
| 12 | | 1 | 5 | 15 | – | – | – | + | + | + | + |
| 13 | Schlenk line | 1 | 5 | 15 | – | + | + | + | + | + | + |

^a[TPE] = 0.134 M (DCM), ^b performed in a glovebox

Acid strength: First, the influence of acid strength was investigated (Entry 1 and 2). The use of weaker trifluoroacetic acid (TFA) instead of HOTf did not give the desired products.

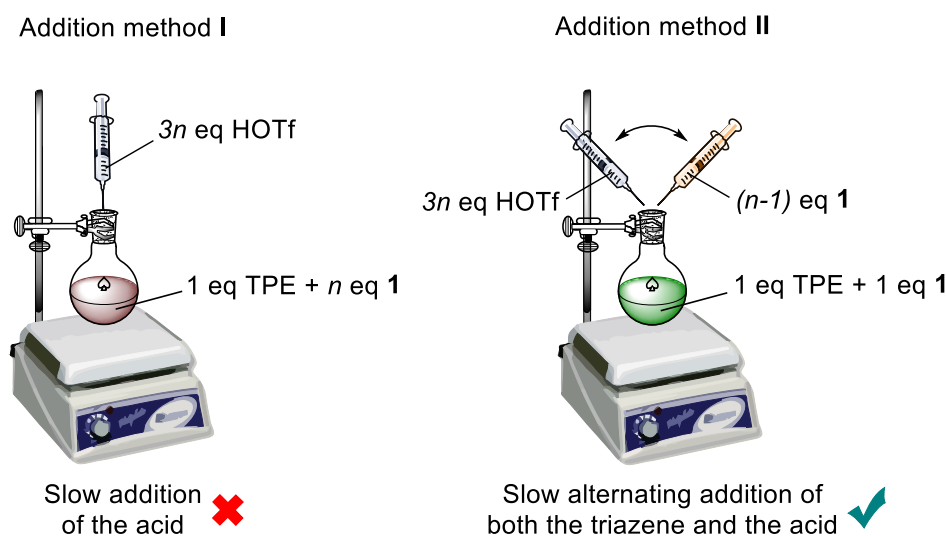
Addition sequence: The polymerization was performed with two different addition sequences, with HOTf (Entry 3) or **1** (Entry 4) being added last to the reaction mixture. The MS results showed that an addition of HOTf after **1** is favorable.

TPE concentration: Subsequently, the influence of the TPE concentration was studied. An excess of TPE (Entry 5) suppressed the formation of oligomers. On the contrary, scaling down the TPE concentration (Entry 6) gave coupling products with $n = 1-4$.

HOTf concentration: Subsequently, the influence of HOTf concentration was investigated (Entry 7 and 8). A pronounced difference was not observed.

Triazene concentration: Increasing the concentration of **1** along with that of HOTf suppressed the coupling reaction (Entry 9 and 10).

Addition method: The experiments using addition method I were performed in the following way: HOTf was added dropwise to a solution of **1** and TPE in DCM (Scheme S2). In the presence of excess **1**, higher oligomers were not observed (Entry 9 and 10). Alternating addition of first **1** and then HOTf followed by stirring for 1 h (method II) gave improved results (Entry 11 and 12).



Scheme S3. The addition methods I and II.

Reconsidering the acid concentration: Using addition method II, the influence of the HOTf concentration was re-evaluated. In experiments with addition method I, the HOTf concentration had a negligible effect (Entry 7 and 8). However, the relative amount of HOTf was found to have an influence when using addition method II (Entry 12). An MS analysis showed that a 3-fold excess of HOTf with respect to the triazene **1** was advantageous.

Glovebox vs. Schlenk line: A polymerization reaction was performed using Schlenk line techniques instead of a glovebox (Entry 13). An MS analysis of the product revealed a higher abundance of products with low masses.

Work-up procedure: The following workup procedure was developed:

1. Addition of dry K_2CO_3 to the reaction mixture and stirring until the color changed from dark green (probably HOTf adducts) to dark orange.
2. Precipitating the products with methanol followed by centrifugation.
3. Washing of the precipitate with methanol to remove phenyl ammonium triflate formed upon cleavage of the triazene group.
4. Washing of the precipitate with a mixture of diethyl ether and hexane (1:1, v/v) to remove shorter oligomers and traces of methanol;

5. Drying under high vacuum at least 3 h.

After applying this work-up procedure for the polymerization with $n = 20$ (**P4**, Scheme S1), an orange amorphous powder was obtained (Fig. S30).



Fig. S34. Photo of a sample of **P4**.

References

- 1 G. R. Fulmer, A. J. M. Miller, N. H. Sherden, H. E. Gottlieb, A. Nudelman, B. M. Stoltz, J. E. Bercaw and K. I. Goldberg, *Organometallics*, 2010, **29**, 2176–2179.
- 2 W. M. Jones and D. D. Maness, *J. Am. Chem. Soc.*, 1970, **92**, 5457–5464.
- 3 G. Pelletier, S. Lie, J. J. Mousseau and A. B. Charette, *Org. Lett.*, 2012, **14**, 5464–5467.
- 4 R. Koller, Q. Huchet, P. Battaglia, J. M. Welch and A. Togni, *Chem. Commun.*, 2009, 5993–5995.
- 5 P. Nimnual, J. Tummatorn, B. Boekfa, C. Thongsornkleeb, S. Ruchirawat, P. Piyachat and K. Punjajom, *J. Org. Chem.*, 2019, **84**, 5603–5613.
- 6 H. Zhou, X. Wang, T. T. Lin, J. Song, B. Z. Tang and J. Xu, *Polym. Chem.*, 2016, **7**, 6309–6317.
- 7 (a) K.-L. Wong, J.-C. Bünzli and P. A. Tanner, *J. Lumin.*, 2020, **224**, 117256; (b) J. R. Lakowicz, *Principles of fluorescence spectroscopy, 3rd Principles of fluorescence spectroscopy*, Springer, New York, USA, 3rd edn, 2006., 2006.
- 8 A. M. Brouwer, *Pure Appl. Chem.*, 2011, **83**, 2213–2228.
- 9 I. M. Smallwood, *Handbook of Organic Solvent Properties*, 1996.
- 10 C. Redshaw, M. R. J. Elsegood, J. W. A. Frese, S. Ashby, Y. Chao and A. Mueller, *Chem. Commun.*, 2012, **48**, 6627–6629.
- 11 M. Zhu, Q. Zhou, H. Cheng, Z. Meng, L. Xiang, Y. Sha, H. Yan and X. Li, *New J. Chem.*, 2022, **46**, 11382–11388.